

# Conductive Gold Nanoparticle Mirrors at Liquid/Liquid Interfaces

*Ping-Ping Fang,<sup>†</sup> Shu Chen,<sup>‡</sup> Haiqiang Deng,<sup>†</sup> Micheál D. Scanlon,<sup>†</sup> Frédéric Gummy,<sup>†</sup> Hye  
Jin Lee,<sup>||</sup> Dmitry Momotenko,<sup>†</sup> Véronique Amstutz,<sup>†</sup> Fernando Cortés-Salazar,<sup>†</sup> Carlos M.  
Pereira,<sup>§</sup> Zhilin Yang<sup>‡</sup> and Hubert H. Girault<sup>\*†</sup>*

<sup>†</sup> Laboratoire d'Electrochimie Physique et Analytique, Ecole Polytechnique Fédérale de  
Lausanne, Station 6, CH-1015 Lausanne, Switzerland.

<sup>‡</sup> Department of Physics, Xiamen University, Xiamen 361005, China.

<sup>||</sup> Department of Chemistry and Green-Nano Materials Research Center, Kyungpook National  
University, 1370 Sankyuk-dong, Buk-gu, Daegu city, 702-701, Republic of Korea.

<sup>§</sup> Centro de Investigação em Química – UP, L4, Departamento de Química e Bioquímica da  
Faculdade de Ciências, Universidade do Porto, 4169-007 Porto, Portugal.

## TABLE OF CONTENTS:

<b>Section</b>		<b>Page</b>
<b>SI-1.</b>	Apparatus to measure Reflectance at a Liquid/Liquid interface	<b>3</b>
<b>SI-2.</b>	Quantification of the Amount of Au NPs Injected at the Interface	<b>4</b>
<b>SI-3.</b>	The Characterization of the Au NPs film by Scanning Electron Microscopy	<b>6</b>
<b>SI-4.</b>	Scanning Electrochemical Microscopy (SECM) assessment of the Au NP film conductivity	<b>8</b>
<b>SI-5.</b>	Cyclic Voltammetry Experiments of a Heptane/DCE solution	<b>10</b>
<b>SI-6.</b>	Schematic of the 3-D Finite Difference Time Domain (FDTD) Calculations of Interfacial Reflectance	<b>11</b>

### SI-1. Apparatus to Measure Reflectance at a Liquid/Liquid interface

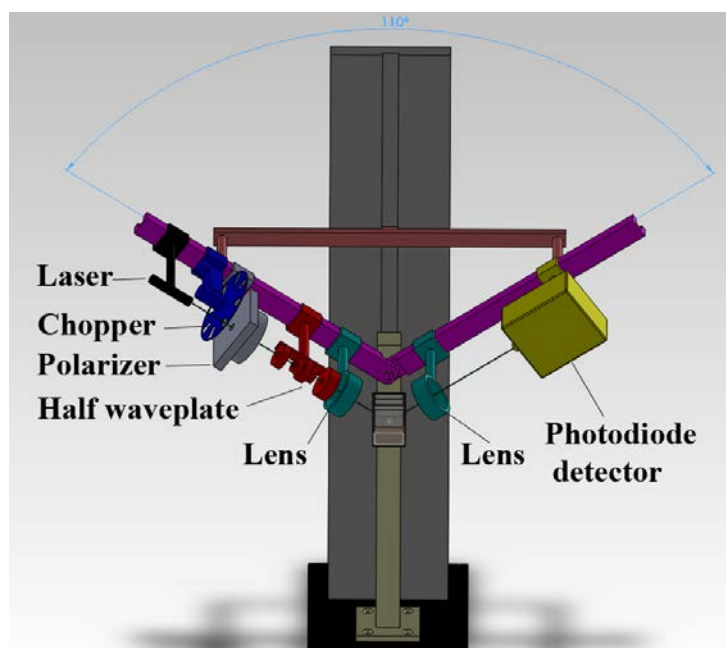


**Figure S1.** Experimental setup employed to study the angular dependence of the reflectance of the Au NP films at the liquid/liquid interface.

To study the angular dependence of the reflectance of the Au NP films at the liquid/liquid interface, on one arm a 532 nm green laser (CPS 532 Collimated Laser Diode Module, Intelite), a chopper, a polarizer, a half wave plate and a focusing lens were mounted, whereas a focusing lens and a photodiode detector were mounted on the other arm, similar to a setup reported elsewhere.<sup>1</sup> The lever in the middle can be moved up and down by the motor, and therefore changes the angle (Figure S1).

## SI-2. Quantification of the amount of Au NPs Injected at the Interface

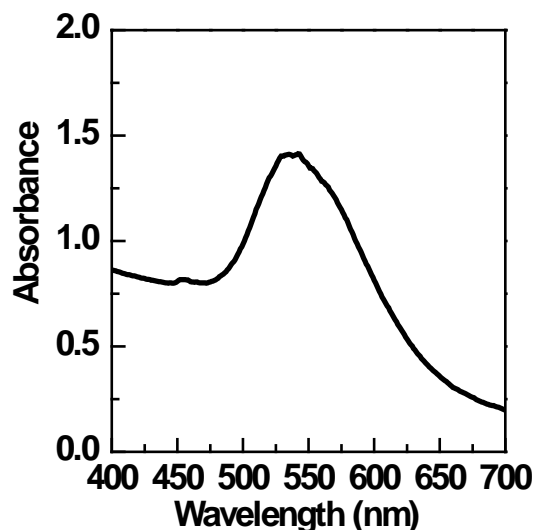


**Figure S2.** UV/visible absorption spectrum of 60 nm Au nanoparticles solution (100  $\mu\text{L}$  of a previously prepared colloidal Au NPs solution + 2 mL of  $\text{H}_2\text{O}$ ).

30 mLs of the colloidal Au NP solution were centrifuged and then dissolved in 0.8 mL ethanol. 100  $\mu\text{L}$  of this solution were dissolved in 2 mL of water and characterised by UV/visible absorption, with the resulting spectrum shown in Figure S2. The concentration and particle size of the Au NP suspensions were calculated from the UV/visible spectra as proposed by Haiss *et al.*<sup>2</sup> Briefly, the wavelength of maximum absorbance ( $\lambda_{\text{max}}$ ) may be correlated with the average particle size. Furthermore, the nanoparticle concentration ( $c$ , mol  $\text{L}^{-1}$ ) can be calculated from the absorbance recorded at 450 nm ( $A_{450}$ ) and the molar extinction coefficient at the same wavelength ( $\epsilon_{450}$ ) for a respective particle size using the Beer-Lambert law:

$$c = \frac{A_{450}}{l\epsilon_{450}} \quad (\text{S1})$$

According to the obtained UV/visible spectra, the average particle size was estimated to be equal to 62 nm ( $\lambda_{\text{max}} = 536.9$  nm). The number of the Au NPs present in a 100  $\mu\text{L}$  aliquot of Au NPs in ethanol was calculated to be ca.  $5.3 \times 10^{10}$  NPs according to the UV/visible spectra (Figure S2) and the  $\epsilon_{450}$  for an average particle size of 62 nm (*i.e.*  $1.91 \times 10^{10} \text{ M}^{-1} \text{ cm}^{-1}$ ).<sup>2</sup> Taking into account the size of the cell (4 cm  $\times$  2 cm), the average size of the nanoparticles, the number of present Au NPs in each 100  $\mu\text{L}$  aliquot Au NP suspension and assuming a square packing structure, about 1.1 equivalent interfacial monolayers (denoted ML) of Au NPs will be formed when 400  $\mu\text{L}$  of the Au NP suspension are injected onto the interface. Analogously, 0.27, 0.41, 0.55, 0.69, 0.82, 0.96, 1.1, 1.2, 1.4, 1.6 ML will be formed when 100, 150, 200, 250, 300, 350, 400, 450, 500, 600  $\mu\text{L}$  of the Au NP suspension are injected onto the interface, respectively. It is important to note that this calculation assumes a flat liquid/liquid interface, which as seen in Figure 2 of the main manuscript is not the case and can lead to an over estimation of the surface coverage. Irrespective, our calculated equivalent interfacial monolayer surface coverage's are good estimations, allowing a more clear comparison between the optical and electrical properties of the prepared Au NPs film.

### SI-3. The Characterization of the Au NPs film by Scanning Electron Microscopy (SEM).

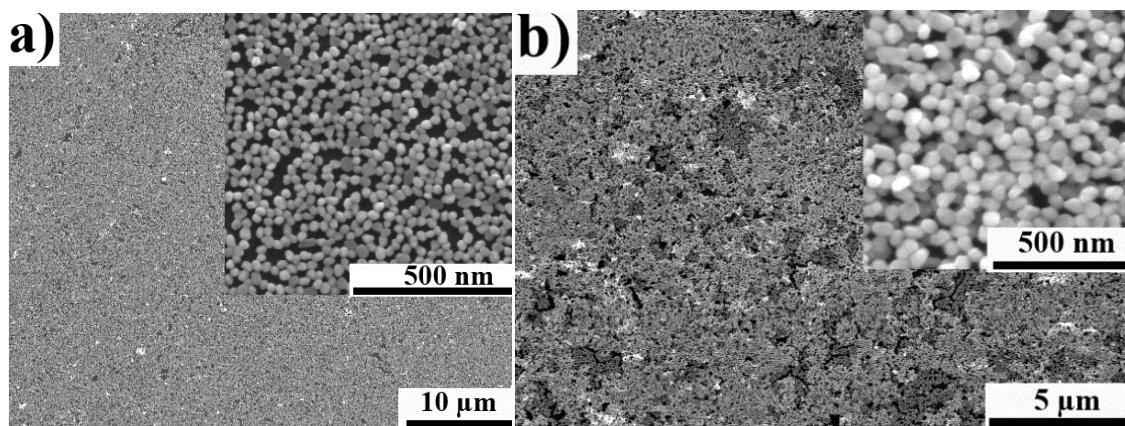


**Figure S3.** SEM images formed with 400  $\mu\text{L}$  (1.1 ML) (a) and 600  $\mu\text{L}$  (1.6 ML) (b) of 60 nm Au NPs in an ethanol solution.

To perform SEM analysis of the Au NP films, an indium tin oxide (ITO) coated glass slide was placed at the bottom of the cell, covered by a thin layer of water and organic phase. Then, a film was formed at the liquid/liquid interface by simply injecting the Au NPs suspended in ethanol. Afterwards, the organic phase was removed carefully using a pipette without disturbing the film. Finally, the ITO glass was slowly taken out from the aqueous phase, dried and used for SEM analysis. Secondary electron images of the Au NPs films investigated were obtained using a Schottky field-emission scanning electron microscope (FEI XLF-30, Philips) operated at beam voltages between 1 and 30 kV. Beam voltages were adjusted to minimize charging effects.

The SEM images of the dried Au NP films showed an almost complete and uniform monolayer of Au NPs were formed when 400  $\mu\text{L}$  of the ethanolic Au NP suspension were injected onto the interface (Figure S3a). According to the UV/visible spectroscopic analysis, the injection of such a volume should lead to the formation of a 1.1 Au NP ML at the interface. The slight difference between the UV/visible and SEM results might be explained

by the loss of Au NPs or the perturbation of its film structure during its preparation for SEM imaging. If more Au NPs are injected onto the liquid/liquid interface, a higher surface coverage and even thicker Au NP films are formed. For instance, a uniform multilayer of Au NP films was formed when 600  $\mu\text{L}$  of the Au NP solution was injected onto the interface, which according to the UV/visible absorption spectra corresponds to 1.6 monolayers (Figure S2). It is expected that the Au NP film at the interface is more uniform, since the perturbations introduced during the drying and extraction of the Au NPs film are avoided. According to the UV/visible spectroscopic and SEM experiments, it can be confirmed that by changing the amount of the Au NPs injected at the interface, a precise control on the amount of self-assembled Au NPs (and thus surface coverage) can be achieved.

#### SI-4. SECM assessment of the Au NPs film Conductivity

The SECM approach curves were done in a typical feedback mode. The water phase has no electrolyte, which is in the bottom part in the cell. The [heptane + DCE] oil phase contains 2 mM DMFc + 2 mM BATB, which is in the top part of the cell. The microelectrode tip was approached to the interface with a scanning rate of  $1 \mu\text{m s}^{-1}$  from the oil phase.

In order to determine the conductivity of the film from the SECM approach curves, it was assumed that the distribution of the surface potential of the conductive film follows the Nernst equation and therefore is a function of the local distribution of the oxidized or reduced forms of the redox mediator employed, in our case DMFc. Then, the measured current is expected to be the result of the interplay of two different processes such as hindrance of the diffusion of the redox mediator towards the surface of the Pt UME and the lateral charge propagation through the film. The measured tip current,  $i_{\text{tip}}$ , is the sum of the component due to hindered diffusion of Red,  $i_{\text{hind}}$ , and the current through the film,  $i_{\text{film}}$  ( $i_{\text{tip}} = i_{\text{hind}} + i_{\text{film}}$ ).

The surface potential difference at the film/solution boundary can be defined by:<sup>3</sup>

$$\begin{aligned} (E_s - E_s^{0'}) = & 137.2146 - 146.3154L - 179.9792I_f + 55.4419(L)^2 + \\ & 115.2713(I_f)^2 + 171.9432LI_f - 7.6379(L)^3 - 22.1172(I_f)^3 - \\ & 112.0059L(I_f)^2 - 67.1270 (L)^2 I_f \end{aligned} \quad (\text{S2})$$

Where  $E_s$  represents the boundary potential between the solution of a redox mediator and the conductive film.  $E_s^{0'}$  stands for the formal potential of the redox couple.  $L$  ( $= d/a$ , probe-substrate distance/radius of the microelectrode) is the normalized tip–film separation and  $I_f = i_{\text{film}}/i_{(\infty)}$  is the normalised lateral film current and  $i_{(\infty)}$  is the steady-state current measured at the bulk of the solution.

$i_{\text{hind}}$  was calculated according to the following equation:<sup>4</sup>



$$i_{\text{hind}} = \frac{2.08 \frac{2.08}{Rg^{0.358}} \left( L - \frac{0.145}{Rg} \right) + 1.585}{2.08 \frac{2.08}{Rg^{0.358}} (L + 0.0023Rg) + 1.57 + \frac{\ln Rg}{L} + \frac{2}{\pi Rg} + \frac{2}{\pi Rg} \ln \left( 1 + \frac{\pi Rg}{2L} \right)} \quad (\text{S3})$$

The resistance of the film,  $R_{\text{film}}$ , can be obtained by plotting  $(E_s - E_s^{0'})$  vs.  $i_{\text{film}}$ , with the data extracted from a single SECM approach curve. Herein, the electrical conductance of the Au NPs film ( $1/R_{\text{film}}$ ) was employed to compare the trend between the optical and electrical properties of the Au NPs film as a function of the surface coverage. A similar protocol was applied for the SECM approach curves performed during this study and presented in Figure 6 of the main document. The estimated electrical conductance is presented in Figure 7 as a function of the amount of Au NPs injected into the liquid/liquid system.

## SI-5. Cyclic Voltammetry Experiments of a Heptane/DCE Solution

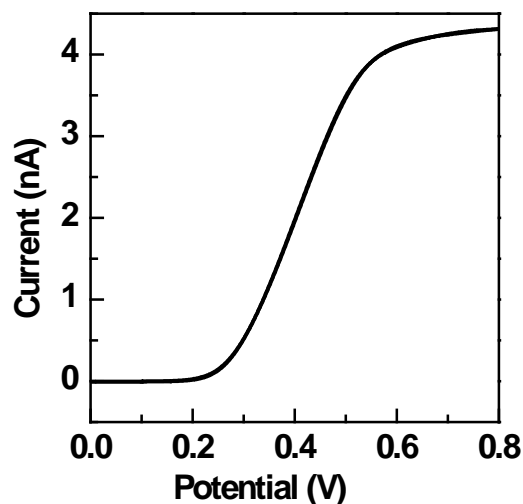


**Figure S4.** Cyclic voltammograms with a 10  $\mu\text{m}$  Pt UME immersed in a 2 mM DMFc + 2 mM BATB heptane/DCE (Volume 3:2) solution.

The electrochemical behaviour of the Pt UME employed during the SECM experiments was tested by cyclic voltammetry in 2 mM DMFc + 2 mM BATB heptane/DCE solution with a distance of about 500  $\mu\text{m}$  between the Pt UME and the Au NPs film. A sigmoidal response was obtained (Figure S4) and latter confirms the possibility to perform SECM experiments at steady-state in the present experimental conditions. A silver/silver chloride wire (Ag/AgCl in 10 mM LiCl + 1 mM BACl aqueous solution) was used as a reference electrode. We choose 0.8 V *vs.* Ag/AgCl as the applied potential to the Pt UME for performing the SECM approach curves.

**SI-6. Schematic of the 3-D Finite Difference Time Domain (FDTD) Calculations of Interfacial Reflectance**

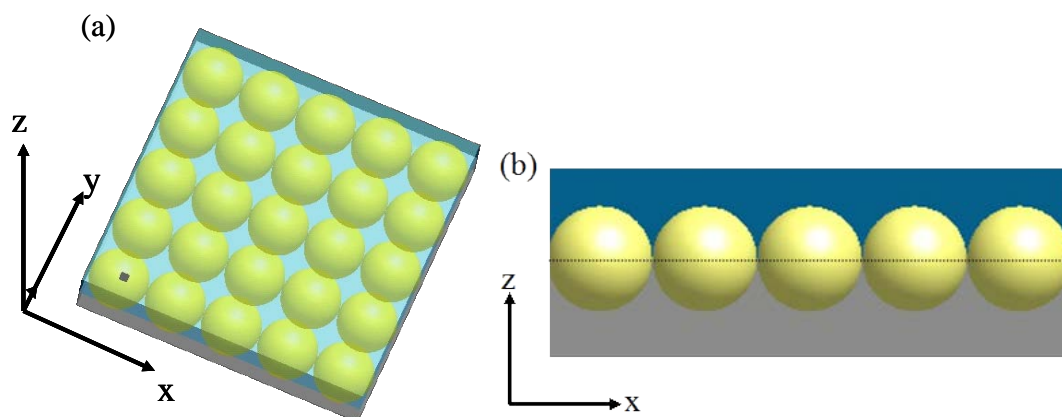


**Figure S5.** Schematic of Au NPs located at [heptane + 1,2-dichloroethane]/water interface forming a film in the  $xy$ -plane. (a) three-dimensional diagram of the calculated model (b) the  $xz$ -plane corresponding to (a).

## References

1. Schaming, D.; Hojeij, M.; Younan, N.; Nagatani, H.; Lee, H. J.; Girault, H. H., Photocurrents at Polarized Liquid|Liquid Interfaces Enhanced by a Gold Nanoparticle Film. *Phys. Chem. Chem. Phys.* **2011**, *13*, 17704-17711.
2. Haiss, W.; Thanh, N. T. K.; Aveyard, J.; Fernig, D. G., Determination of Size and Concentration of Gold Nanoparticles from UV-Vis spectra. *Anal. Chem.* **2007**, *79*, 4215-4221.
3. Whitworth, A. L.; Mandler, D.; Unwin, P. R., Theory of Scanning Electrochemical Microscopy (SECM) as a Probe of Surface Conductivity. *Phys. Chem. Chem. Phys.* **2005**, *7*, 356-365.
4. Cornut, R.; Lefrou, C., New Analytical Approximation of Feedback Approach Curves with a Microdisk SECM tip and Irreversible Kinetic Reaction at the Substrate. *J. Electroanal. Chem.* **2008**, *621*, 178-184.